

# RESEARCH/INVESTIGACIÓN

## MORPHOLOGICAL AND MOLECULAR CHARACTERIZATION OF A POPULATION OF *PRATYLENCHUS HIPPEASTRI* (NEMATODA-PRATYLENCHIDAE) PARASITIZING MUSCADINE GRAPE IN FLORIDA

A. Habteweld\*, C. Bania, and W. T. Crow

Department of Entomology and Nematology, University of Florida, Gainesville, FL 32611, USA;

\*Corresponding author: [ahabteweld@ufl.edu](mailto:ahabteweld@ufl.edu)

---

### ABSTRACT

Habteweld, A., C. Bania, and W. T. Crow. 2021. Morphological and molecular characterization of a population of *Pratylenchus hippeastri* (Nematoda-Pratylenchidae) parasitizing muscadine grape in Florida. *Nematropica* 51:56-66.

Root-lesion nematodes are among the most prevalent nematodes that can infect and cause damage to grapevine roots. Females and juveniles of a *Pratylenchus* sp. were extracted from composite root samples collected from muscadine grape (*Vitis rotundifolia*) in a vineyard in central Florida. Morphological observations and molecular analysis of 28S large subunit ribosomal DNA and mitochondrial cytochrome oxidase I (COI) sequences of this population indicated that it was a representative of the amaryllis root-lesion nematode, *Pratylenchus hippeastri*. To our knowledge, this represents the first report of *P. hippeastri* on muscadine grape. Morphological characters of the population from muscadine grape in Florida were consistent with those in the original description for the species except for slight variation in the ratio b' [4.5 (3.7-5.9) vs 3.9 (3.6-4.3); mean (range)] and excretory pore distance from anterior end [85.0 (84.7-101.0) vs 91.0 (85.0-95.0)  $\mu\text{m}$ ]. The Florida population from muscadine grape had longer body length (588 (478.0-668.0)  $\mu\text{m}$ ) than that of other populations previously recovered from apple in China (447.8 (400.7-479.8)  $\mu\text{m}$ ) and European grape (*Vitis vinifera*) in California (436.0 (402.0-476.0)  $\mu\text{m}$ ). The occurrence of *P. hippeastri* on muscadine grape and other hosts reported outside Florida suggests that this species has a wide host and geographical range.

*Key words:* Amaryllis root lesion nematode, COI mtDNA gene, D2-D3 of 28S rRNA gene, diagnosis, morphometrics, phylogenetic analysis

---

### RESUMEN

Habteweld, A., C. Bania, y W. T. Crow. 2021. Caracterización morfológica y molecular de una población de *Pratylenchus hippeastri* (Nematoda-Pratylenchidae) parasitando la vid muscadine en Florida. *Nematropica* 51:56-66.

Los nematodos lesionadores de raíces se encuentran entre los nematodos más prevalentes que pueden infectar y dañar las raíces de la vid. Juveniles y hembras de un *Pratylenchus* sp. fueron extraídos de muestras compuestas de raíces recolectadas de la vid muscadine (*Vitis rotundifolia*) en un viñedo en Florida Central. Observaciones morfológicas y análisis moleculares del 28S subunidad mayor del ADN ribosomal y

secuencias del citocromo oxidasa I (COI) de ADN mitocondrial de esta población indicó que fue representativa del nematodo lesionador del amarillis *Pratylenchus hippeastri*. A nuestro conocimiento, este es el primer informe de *P. hippeastri* en vid muscadine. Caracteres morfológicos de la población en vid muscadine en Florida fue consistente con aquellos en la descripción original para la especie excepto por una ligera variación en el radio b' [4.5 (3.7-5.9) vs 3.9 (3.6-4.3); promedio (rango)] y la distancia del poro excretor desde la parte anterior del nematodo [85.0 (84.7-101.0) vs 91.0 (85.0-95.0)  $\mu\text{m}$ ]. La población del nematodo en vid muscadine de la Florida presentó una longitud del cuerpo más larga (588 (478.0-668.0)  $\mu\text{m}$ ) que aquellas otras poblaciones previamente recuperadas de manzana en China (447.8 (400.7-479.8)  $\mu\text{m}$ ) y la vid Europea (*Vitis vinifera*) en California (436.0 (402.0-476.0)  $\mu\text{m}$ ). La ocurrencia de *P. hippeastri* en vid muscadine y otros hospederos reportados fuera de Florida sugieren que esta especie posee un amplio rango de hospederos y geográfico.

*Palabras clave:* El nematodo lesionador del amarillis, gen COI del ADNmt, D2-D3 del gen 28S del ARNr, diagnóstico, morfometría, análisis filogenético

## INTRODUCTION

Two species of grape, European bunch grape (*Vitis vinifera* L.) and muscadine grape (*V. rotundifolia* Michx), are grown in Florida. However, due to susceptibility of *V. vinifera* to Pierce's disease caused by *Xylella fastidiosa*, which is widespread in Florida, only the native and resistant muscadine grape is commonly cultivated in the State (Anderson *et al.*, 2003). Plant-parasitic nematodes are one of the biotic factors damaging grapevine production in Florida by transmitting viruses, weakening vines, and debilitating their root system (Crow and Rich, 2006). Root lesion nematodes (*Pratylenchus* spp.) are among the most prevalent nematodes that can infect and cause damage to the grape roots (Téliz *et al.*, 2007; Howland *et al.*, 2014). During a class project in 2020, composite root samples from muscadine grape were collected in central Florida and found infected with a root lesion nematode population resembling *Pratylenchus hippeastri* Inserra, Troccoli, Gozel, Bernard, Dunn, and Duncan, 2007. This species was originally described from roots of *Hippeastrum* sp. (amaryllis) in Florida (Inserra *et al.*, 2007). The identification of this nematode is challenging and requires the morphological examination of many specimens and corroboration with molecular analyses.

Since there are no records of infections of *P. hippeastri* on muscadine grapes, a study was conducted to: (i) characterize the population of *P. hippeastri* recovered from muscadine grape roots in Florida using morphometrics and molecular DNA barcoding and (ii) determine the phylogenetic relationship of this root lesion

nematode population with other related species based on the D2-D3 expansion segments of 28S rRNA and partial COI mtDNA gene sequences.

## MATERIALS AND METHODS

### *Nematode population, extraction, and morphological characterization*

Muscadine grape root samples from three vines in the same field were collected from Clermont, Lake County in Florida, and transported to UF/IFAS Nematode Assay Laboratory (Gainesville, FL) for nematode diagnosis in November 2020. The roots were mixed together to form a composite root sample and washed with distilled water to remove soil from the root surface. Nematodes were extracted from 10 g of moist roots incubated in a mist chamber for 72 hr (Crow *et al.*, 2020). In total, 10 females were used for morphometric characterization. Nematodes were processed for permanent mounting according to Habteweld *et al.* (2019). The specimens were examined for morphological features and morphometrics using a camera installed on an Olympus BH-2 microscope (Olympus, Japan). Measurements were taken using the ZEN lite software on ZEISS Axiocam ERc5s digital camera (Zeiss, Oberkochen, Germany). Morphological and morphometric characteristics of *P. hippeastri* were compared with those of the paratypes in the original description (Inserra *et al.*, 2007) and other *P. hippeastri* populations (De Luca *et al.*, 2010; Gu *et al.*, 2014; Wang *et al.*, 2016; Shokoohi *et al.*, 2019; Knoetze *et al.*, 2019; Handoo *et al.*, 2020).

### *Molecular characterization and phylogenetic relationships*

Total genomic DNA was extracted following the proteinase K method as described by Pagan *et al.* (2015). A single female was transferred to a DNA extraction buffer containing 18  $\mu$ l Tris-EDTA buffer, 1  $\mu$ l of 2% triton, and 1  $\mu$ l of proteinase K (20 mg/ml). The nematode in the extraction buffer was frozen and thawed four times and placed at  $-20^{\circ}\text{C}$  overnight. The DNA was extracted by incubating the tube at  $56^{\circ}\text{C}$  for 1 hr followed by deactivation at  $95^{\circ}\text{C}$  for 15 min using T100TM thermocycler (Bio-Rad Laboratories, Inc., Hercules, CA). DNA amplification was performed in 25  $\mu$ l of reaction mix containing 12.5  $\mu$ l  $2\times$  Hot Start Master mix (Genessee Scientific, San Diego, CA), 0.75  $\mu$ l forward and reverse primers, 2  $\mu$ l sterile nuclease free water (Thermo Fisher Scientific, Gainesville, FL), and 9  $\mu$ l template DNA. D2-D3 expansion segment of the large subunit (LSU) rDNA was amplified using the primer sets D2A (5'-CAAGTACCGTGAGGGAAAGTTG-3') and D3B (5'-TCGGAAGGAACCAGCTACTA-3') (De Ley *et al.*, 2005). Mitochondrial cytochrome oxidase I (COI) was amplified with JB3 (5'-TTTTTTGGGCATCCTGAGGTTTAT-3') and JB5 (5'-AGCACCTAACTTAAAACATAATGAAAATG-3') (Derycke *et al.*, 2005). The thermocycling reactions for both DNA regions were as follows:  $95^{\circ}\text{C}$  for 15 min, followed by 38 cycles of  $94^{\circ}\text{C}$  for 30 sec,  $55^{\circ}\text{C}$  for 45 sec, and  $72^{\circ}\text{C}$  for 1 min, and a final extension step of  $72^{\circ}\text{C}$  for 7 min. PCR clean-up and sequencing were performed by Genewiz LLC (South Plainfield, NJ).

The COI mtDNA and the 28S rRNA D2-D3 expansion segment genes were sequenced from two and one individual females, respectively. To identify the species, raw sequences were checked and edited manually using Geneious Prime 2020.2.5 (Auckland, New Zealand). Consensus sequences obtained were compared with those deposited in the GenBank database using BLAST engine search for sequence identity. The newly obtained sequences were submitted to GenBank database under accession numbers MZ355925 for D2-D3 of the 28S rRNA gene, and MZ355922 and MZ355923 for COI. To perform the phylogenetic analysis, D2-D3 LSU and COI sequences obtained from *P. hippeastri* identified in the present study

and those retrieved from GenBank databases were aligned over the same length in MUSCLE using MEGA v. X (Kumar *et al.*, 2018) (Figs. 1, 2). The alignment was analyzed to obtain the base substitution model for these sequences using MEGA X (Kumar *et al.*, 2018). For both D2-D3 LSU and COI sequences, the evolutionary history was inferred by using the maximum likelihood method and Tamura-Nei model (Tamura and Nei, 1993). Initial tree(s) for the heuristic search were obtained automatically by applying neighbor-joining and BioNJ algorithms to a matrix of pairwise distances estimated using the maximum composite likelihood (MCL) approach, and then selecting the topology with superior log-likelihood value. The phylogram was generated using base substitution model selected for each alignment and running maximum likelihood model with 1,000 bootstrap replicates using MEGA X to assess the degree of support for each branch on the tree (Landa *et al.*, 2008).

## RESULTS

### *Morphometric characterization*

The root lesion nematode population extracted from muscadine grape roots consisted of females and juveniles only. No males were found. The morphometric characters of females were consistent with those given for the type population by Inserra *et al.* (2007) (Table 1).

### *Molecular characterization and phylogenetic relationships*

The sequencing of the PCR product amplified using D2A and D3B primers yielded a product of approximately 768 bp in length. D2-D3 expansion segment of the 28S rRNA gene from the population in the present study showed  $>96\%$  similarity with *P. hippeastri* sequences from NCBI GenBank including those from amaryllis in Florida (DQ498829), bottlebrush (*Callistemon rigidus*) in Florida (GU131130) and Japanese Maple (*Acer palmatum*) in Japan (KC796706). The D2-D3 alignment included 34 sequences and had 670 positions in length in the final dataset. Out of the 33 sequences, 16 of them were from *P. hippeastri* from GenBank and one sequence was from the present study (Fig. 1). The D2-D3 of 28S rRNA gene sequence of *P. hippeastri* in the present study

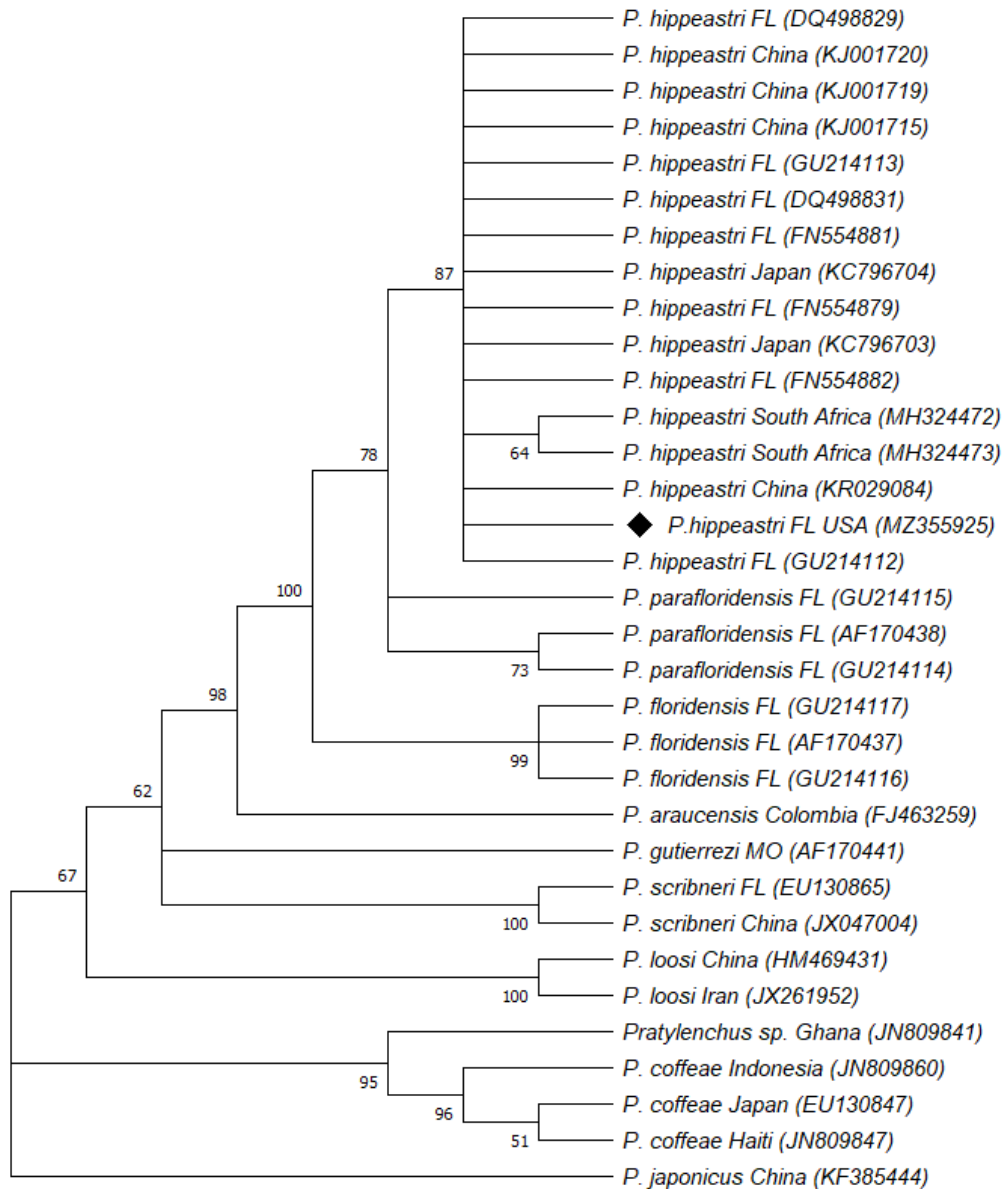


Figure 1. Phylogenetic relationship based on D2-D3 expansion segments of 28S rRNA gene sequences of a *P. hippeastri* population from muscadine grape with closely related species within the genus *Pratylenchus*. The evolutionary history was inferred by using the maximum likelihood method and Tamura-Nei model (Tamura and Nei, 1993). The tree with the highest log likelihood (-2642.14) is shown. The percentage of trees in which the associated taxa clustered together is shown next to the branches. Initial tree(s) for the heuristic search were obtained automatically by applying Neighbor-Join and BioNJ algorithms to a matrix of pairwise distances estimated using the maximum composite likelihood (MCL) approach, and then selecting the topology with superior log likelihood value. This analysis involved 33 nucleotide sequences. There was a total of 670 positions in the final dataset. Evolutionary analyses were conducted in MEGA X (Kumar et al., 2018). Accession preceded by ◆ is a new sequence.

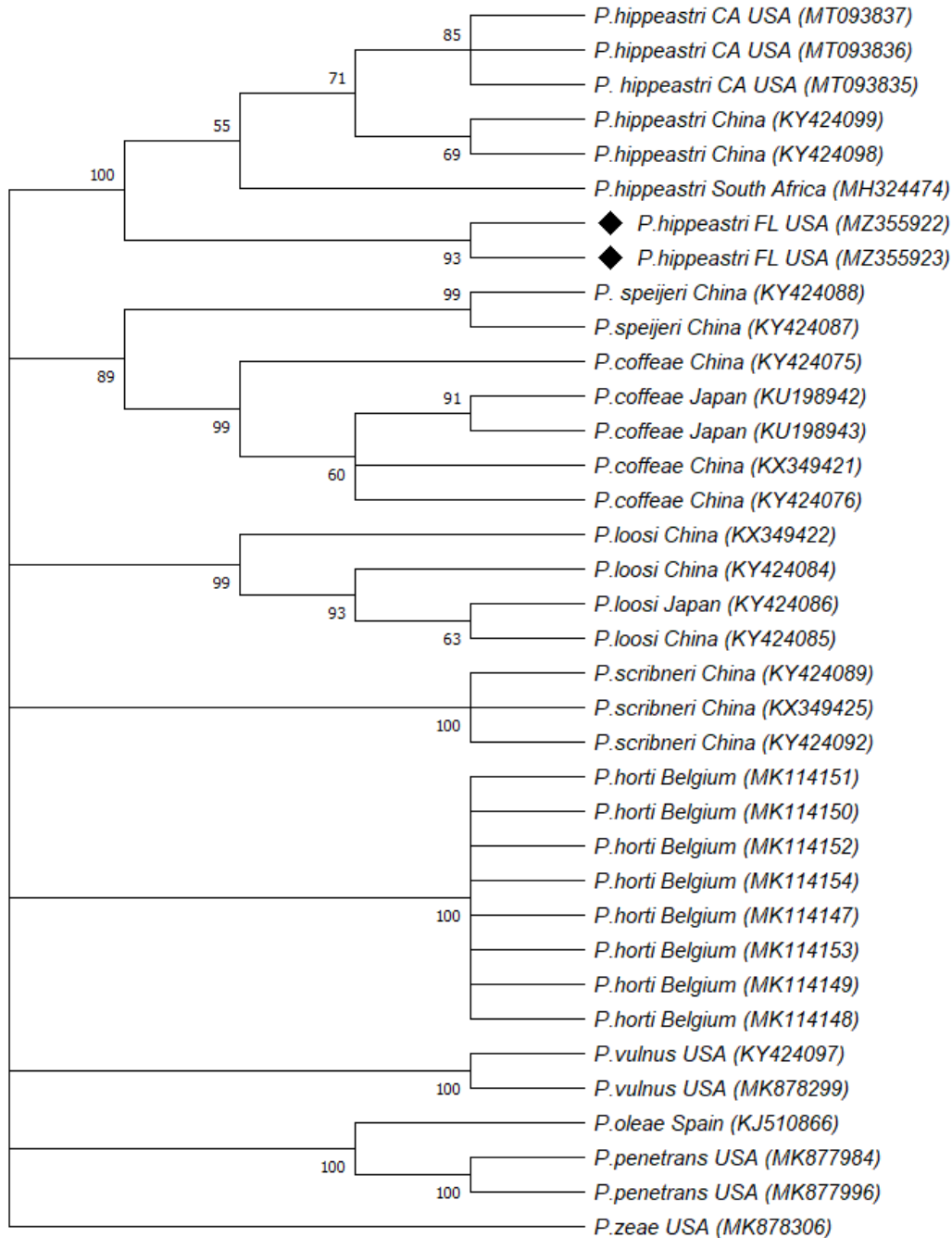


Figure 2. Phylogenetic relationship based on COI mtDNA gene sequences of a *P. hippeastri* population from muscadine grape with closely related species within the genus *Pratylenchus*. The evolutionary history was inferred by using the maximum likelihood method and Tamura-Nei model (Tamura and Nei, 1993). The tree with the highest log likelihood (-2873.13) is shown. The percentage of trees in which the associated taxa clustered together is shown next to the branches. Initial tree(s) for the heuristic search were obtained automatically by applying Neighbor-Join and BioNJ algorithms to a matrix of pairwise distances estimated using the maximum composite likelihood (MCL) approach, and then selecting the topology with superior log likelihood value. This analysis involved 36 nucleotide sequences. Codon positions included were 1st+2nd+3rd+Noncoding. There was a total of 357 positions in the final dataset. Evolutionary analyses were conducted in MEGA X (Kumar *et al.*, 2018). Accessions preceded by ♦ are new sequences.

Table 1. Morphometrics of females of *Pratylenchus hippocastri* populations from the present and previous studies.

	Present study	Inserra et al. (2007)	De Luca et al. (2012)	Gu et al. (2014)	Wang et al. (2016)	Shokoohi et al., 2019	Snoetze et al. (2019)	Handoo et al. 2020
n	10	22	10	16		7	36	10.0
L	588.0 ± 57.0	590 ± 21.8	614.0±22.4	479.9±31.9	447.8±28.2	522.6 ± 69.5	510.0 ± 37.7	436.0
a	(478.0-668.0) 24.7± 4.1	(545-627) 25.5±1.2	(585.0-651.0) 25.2±2.0	(418.0-526.0) 28.0±1.9	(400.7-479.8) 27.7±1.4	(424.0-614.0) 28.5 ± 3.1	(408-598) 27.1 ± 2.4	(402.0-476.0) 25.0
b	(19.1-32.0) 6.0±1.0	(23.2-27.9) 6.5 ± 0.4	(23.7-26.5) 6.6±0.4	(25.5-32.2) 6.2±0.3	(25-29.1) 5.4±0.3	(18.6-31.8) 3.8 ± 0.7	(21.4-32.4) 4.1 ± 0.3	(20.0-32.0) 4.2
b'	(4.8-7.7) 4.5±0.8	(5.7-7.1) 3.9 ± 0.2	(5.9-7.2) 4.5±0.4	(5.7-6.7) 3.9±0.3	(5.0-5.8) 3.2±0.2	(2.7-4.9) -	(3.6-4.7) 5.5 ± 0.4	(3.6-4.7) -
c	(3.7-5.9) 15.9±1.9	(3.6-4.3) 16.1±1.0	(4.0-5.3) 18.6±2.0	(3.4-4.5) 16.5±1.3	(2.8-3.5) 17.9±1.5	(5-6.6) 18.7 ± 3.1	(5-6.6) 17.7 ± 1.8	(5-6.6) 17.0
c'	(13.2-18.8) 2.6±0.5	(14.6-18.7) 2.6 ± 0.2	(16.4-23.3) 2.2±0.2	(13.6-18.4) 2.7±0.3	(15.6-20.5) 2.3±0.2	(11.7-23.6) 2.2 ± 0.2	(14.4-22.5) 2.3 ± 0.3	(15.0-21.0) 2.1
V	(1.8-3.3) 76.0±2.8	(2.2-2.9) 77.0 ± 0.8	(1.8-2.5) 77.7±1.2	(2.2-3.4) 77.2±1.0	(1.9-2.5) 78.2±1.3	(2.0-2.3) 77.1 ± 3.5	(1.7-3.3) 77 ± 1.9	(1.6-2.5) 77.0
Stylet length	(73.0-82.0) 16.7±0.6	(75.0-78.0) 15.5 ± 0.4	(75.7-79.4) 15.8±0.4	(75.0-79.6) 15.8±0.8	(76.4-80.2) 14.9±0.4	(73-82) 15.4 ± 1.6	(71-81.2) 15 ± 0.6	(74.0-79.0) 15.0
Stylet shaft	(15.8-17.3) 6.8±0.4	(15.0-16.0) -	(15.3-16.7) -	(14.5-17.5) -	(14.4-15.6) 7.4±0.2	(13-18) 4.9 ± 1.2	(14-16) -	(13.0-15.5) -
Stylet knob width	(5.5-6.6) 4.0±0.5	4.7 ± 0.3	-	-	(7.1-7.6) 3.2±0.2	(4.2-5.8) 3.4 ± 0.7	4 ± 0.4	-
Stylet knob height	(3.5-5.1) 2.6±0.3	(4.0-5.0) 2.1 ± 0.3	-	-	(2.9-3.5) 1.8±0.1	(2.7-4.1) 2.2 ± 0.4	(3-5) 2.5 ± 0.3	-
DGO from stylet base	(2.1-3.0) 2.9±0.3	(1.5-3.0) 2.9 ± 0.2	-	-	(1.6-1.9) 2.8±0.2	(1.7-2.5) 2.7 ± 0.9	(2-3) 3 ± 0.6	-
	(2.3-3.2) 2.3±0.3	(2.5-3.0) 2.5±0.3	(2.0-2.7) 2.7±0.4	(2.1-3.3) 2.1±0.3	(2.5-3.2) 2.5±0.3	(1.7-3.6) 2.7 ± 0.9	(2-4) 3 ± 0.6	-

Table 1. Continued.

	Present study	Inserra <i>et al.</i> (2007)	De Luca <i>et al.</i> (2012)	Gu <i>et al.</i> (2014)	Wang <i>et al.</i> (2016)	Shokoohi <i>et al.</i> , 2019	Snoetze <i>et al.</i> (2019)	Handoo <i>et al.</i> 2020
<b>Anterior end to:</b>								
Centre of metacarpus	59.1±12 (41.0-77.0)	63 ± 1.9 (59-66)	62.0 ± 1.9 (58.0-65.0)	52.6±2.6 (48.9-58.0)	53.7±2.4 (50.0-57.0)	–	–	–
Cardia	–	92 ± 3.3 (83-98)	93.0 ± 5.3 (87.0-106.0)	–	83.3±3.2 (79.4-89.9)	–	–	–
End of pharyngeal gland lobe	131.0±18.0 (109.0-168.0)	134.0 ± 6.6 (116.0-145.0)	137.0± 8.8 (123.0-147.0)	–	138.9±6.1 (126.3-148)	132.9 ± 15.9 (116-149)	–	104.0 (98.0-111.0)
Excretory pore	85.0±12.1 (84.7-101.0)	91.0 ± 2.5 (85.0-95.0)	94.0±2.9 (89.0-99.0)	78.1±4.6 (70.9-84.8)	79.2±2.7 (74.9-83.1)	95.7 ± 15.1 (80-112)	–	–
Pharyngeal overlap	31.4±5.1 (25.0-41.0)	43.0 ± 5.4 (32.0-51.0)	44.5 ± 7.6 (33.0-58.0)	47.1±6.7 (37.6-57.9)	54.9±5.4 (44.5-64)	32-43	31 ± 6 (21-48)	–
Max. body diam.	23.4±2.2 (20.0-26.4)	23.2 ± 1.4 (21.0-27.0)	24.4±0.7 (23.3-25.7)	17.2±1.7 (14.3-20.0)	16.2±0.9 (14.6-17.6)	20.9 ± 3.4 (17-27)	19 ± 1.5 (16-21)	20.0 (15.0-28.5)
Vulval body diam.	18.6±2.3 (16.0-22.0)	20.5±1.1 (18.0-23.0)	21.6 ± 1.6 (19.3-24)	15.6±1.7 (12.7-18.5)	14.9±1 (13.3-16.2)	–	–	–
Anal body diam.	14.2±1.7 (12.0-17.0)	14.4 ± 0.8 (13.0-16.0)	15.3 ± 0.4 (14.7-16)	11.4±1.2 (10.2-13.2)	11.0 ± 0.7 (9.5-12.1)	12.9 ± 1.0 (12-14)	13 ± 1.1 (11-17)	12.0 (10.5-13.0)
Spermatheca-vagina	–	45.0 ± 9.5 (32.0-71.0)	–	42.2±9.6 (33.4-58.4)	28.6±2.5 (26.5-34.1)	–	–	–
Tail length	37.5±4.1 (29.0-43.0)	36.8±2.2 (32.0-42.0)	33.3 ± 3.0 (28.0-37.3)	29.5±3.1 (25.0-34.4)	25±1.9 (21.3-27)	31.7 ± 6.4 (26-43)	29 ± 2.1 (24-36)	26.0 (21.0-29.0)
No. of tail annuli	–	22.0 ± 2.1 (19.0-26.0)	24.0 ± 1.9 (21.0-26)	21.3±2.2 (17.0-25.0)	22.8±1.6 (21.0-26.0)	21.3 ± 2.8 (18.0-23.0)	23 ± 1 (18.0-34.0)	–
Vulva to anus distance	104.4±10 (88.0-119.0)	98.0 ± 6.1 (88.0-112.0)	103.0 ± 5.4 (92.0-109.0)	77.0±9.8 (65.393.6)	74.4±8.6 (61.5-85.1)	77.5 ± 7.7 (72.0-83.0)	120 ± 12.2 (89.0-147.0)	–
Post-uterine sac	29.2±7.5 (20.0-45.0)	30.0 ± 4.9 (21.0-45.0)	34.5 ± 3.0 (30.0-39.3)	24.0±2.8 (19.0-27.2)	22.2±3.1 (19.5-27.6)	20.6 ± 3.9 (16.0-26.0)	29.0 ± 4.9 (20.0-39.0)	–

Table 1. Continued.

	Present study	Inserra <i>et al.</i> (2007)	De Luca <i>et al.</i> (2012)	Gu <i>et al.</i> (2014)	Wang <i>et al.</i> (2016)	Shokoohi <i>et al.</i> , 2019	Snoetze <i>et al.</i> (2019)	Handoo <i>et al.</i> 2020
Lateral field width	-	-	-	-	5.3±0.4	5.5 ± 0.7 (5.0–6.0)	-	-
Phasmids from tail terminus	-	-	-	-	11.9±1 (10.5-14.2)	-	-	-
E.P. (%)	-	-	-	-	17.7±0.7 (16.9-19.1)	-	-	-
Lip width	8.7±0.6 (7.2-9.2)	-	-	-	7.1±0.3 (6.6-7.4)	-	7 ± 1.4 (7.5-9)	-
Lip height	2.8±0.3 (2.4-3.4)	-	-	-	2±0.2 (1.6-2.2)	-	2.5 ± 0.2 (2-3)	-

“-” data not available.

differed by 19-23 nucleotides (2.8-3.4%) from *P. hippeastri* populations from GenBank. Phylogenetic analysis inferred from the D2-D3 region placed *P. hippeastri* population from the present study and all *P. hippeastri* sequences obtained from GenBank in a highly (87%) supported clade, which was nearest to that of *P. parafloridensis* and *P. floridensis* (Fig. 1).

The sequencing of the PCR product amplified with JB3 and JB5 primers yielded a product of approximately 442 bp in length for COI gene. Based on BLASTN analysis, the COI gene of the population showed 98% identity with *P. hippeastri* sequences from NCBI GenBank including those from apple in South Africa (MW042870), European bunch grape in California (MT093836) and population from China (KY424099). The COI alignment included 36 sequences and had 357 positions in length. Out of the 36 sequences 34 were obtained from GenBank and 2 sequences were obtained from the present study. COI gene sequences from the present study differed by 7-8 nucleotides (1.7-2.3%) from *P. hippeastri* sequences from GenBank except for a sequence from South Africa (MW042870), which differed by 12 nucleotides (3.1%). No nucleotide differences were observed between the two COI gene sequences obtained from the present study. The phylogenetic analysis of COI sequences from the present study and those obtained from GenBank grouped together with maximal support (100%). In the COI tree, *P. hippeastri* clustered in a clade close to that of *P. speijeri* (Fig. 2). Unfortunately, the relationship among the *P. hippeastri* population from muscadine grape and *P. hippeastri* paratypes, *P. parafloridensis* and *P. floridensis* could not be elucidated with this analysis because no COI gene sequences for these three species are available in GenBank. The results of the two phylogenetic analyses validate those of the morphological analysis confirming that the Florida population of the root lesion nematode from muscadine grape is *P. hippeastri*. This is a new host record for this species.

## DISCUSSION

In the present study, morphometric and morphological characters of *P. hippeastri* from muscadine grape in Florida were consistent with the original description except slight variation in b' [4.5 (3.7-5.9) vs 3.9 (3.6-4.3); mean (range)] and

excretory pore distance from anterior end (85.0 (84.7-101.0) vs 91.0 (85.0-95.0)  $\mu\text{m}$ ) (Inserra *et al.*, 2007). Body length was greater (588 (478.0-668.0)  $\mu\text{m}$ ) than that of the populations recovered from apple in China (447.8 (400.7-479.8)  $\mu\text{m}$ ) (Wang *et al.*, 2016) and European bunch grapevine in California (436.0 (402.0-476.0)  $\mu\text{m}$ ) (Handoo *et al.*, 2020) (Table 1). The population from the present study also differed in the ratio b' (4.5 (3.7-5.9) vs 3.2 (2.8-3.5)), stylet shaft length (6.8 (5.5-6.6) vs 7.4 (7.1-7.6)  $\mu\text{m}$ ), stylet knob height (2.6 (2.1-3.0) vs 1.8 (1.6-1.9)  $\mu\text{m}$ ) and excretory pore distance from anterior end (85 (84.7-101.0) vs 79.2 (74.9-83.1)  $\mu\text{m}$ ) from the population recovered from apple in China (Wang *et al.*, 2016), and in the last character (85 (84.7-101.0) vs 78.1 (70.9-84.8)  $\mu\text{m}$ ) from the population recovered from the rhizosphere of apple in Japan (Gu *et al.*, 2014).

Reports indicated that morphometric characters within a species may be influenced by nutrient availability or other environmental conditions (Castillo and Vovlas, 2007; Janssen *et al.*, 2017). Female body length of *P. coffeae* isolated from citrus was found to be seasonal and correlated with the starch content in the fibrous roots of the host (Duncan *et al.*, 1998). This morphological variability can complicate the identification of root-lesion nematodes (Castillo and Vovlas, 2007; Janssen *et al.*, 2017).

*Pratylenchus hippeastri* was described as a closely related species of *P. scribneri*. These species are morphologically separated by the configuration of the lip patterns observable using scanning electron microscopy; lips are fused in *P. hippeastri*, but they are divided in *P. scribneri*. Minor differences, however, separate these two species under light microscopy (Inserra *et al.*, 2007). *Pratylenchus hippeastri* differed from *P. scribneri* Steiner, 1943 by a longer tail length (36.6 (30.8-43.1) vs 26.7 (21.5-29.6)  $\mu\text{m}$ ), slightly longer stylet (15.5 (15.0-16.0) vs 14.6 (14.0-15.5)  $\mu\text{m}$ ), and shape of tail terminus (often bluntly pointed and smooth vs the consistently hemispherical and smooth tail terminus) (Inserra *et al.*, 2007). Interspecific overlap in these characters between *P. hippeastri* and *P. scribneri* has been observed more frequently in *P. hippeastri* populations that have been reported in many geographical areas after the original description.

De Luca *et al.* (2010) considered *P. hippeastri*, *P. floridensis*, and *P. parafloridensis* isolated from Florida as the 'hippeastri' species

complex. *Pratylenchus floridensis* and *P. parafloridensis* differ from *P. hippeastri* in spermatheca and tail end morphology. The spermatheca in *P. hippeastri* is considered as non-functional while functional in *P. floridensis* and *P. parafloridensis*. Tail end morphology is almost indented in *P. hippeastri*, but almost smooth in *P. floridensis* and *P. parafloridensis* (De Luca et al., 2010). However, it is difficult to reliably separate *P. hippeastri* from closely related species based only on morphology, therefore, molecular characters become more relevant for differentiating these species.

The D2-D3 expansion segment of 28S rRNA and COI mtDNA genes of the population in the present study showed >96% and >98% identities with *P. hippeastri* sequences from NCBI GenBank for D2D3 and COI genes, respectively. The intraspecific variability of the D2-D3 segment of the 28S rRNA in the present study and sequences from GenBank was relatively high (2.8-3.4%). In contrast, this intraspecific variability was small (1.7-2.3%) for COI mtDNA gene. Phylogenetic trees inferred from alignments of D2-D3 and COI genes placed the Florida population from grapevine within the monophyletic group of *P. hippeastri*. The phylogenetic tree generated from the D2-D3 region also placed the *P. hippeastri* population nearest to *P. parafloridensis* and *P. floridensis* in agreement with prior studies (De Luca et al., 2010; Wang et al., 2016; Handoo et al., 2020). The pairwise genetic distance of these three species revealed that *P. hippeastri* from the present study has 0.035 and 0.04 difference with *P. parafloridensis* and *P. floridensis*, respectively, while 0.12 between *P. scribneri*. However, the phylogenetic tree generated from COI gene placed the Florida population nearest to *P. speijeri* as there are no COI sequences for *P. hippeastri* paratypes, *P. parafloridensis* and *P. floridensis* in GenBank.

Based on morphometric characters and molecular analyses, we identified the population from muscadine grape in Florida as *P. hippeastri*. To our knowledge, this finding represents the first report of the amaryllis lesion nematode on muscadine grape (*V. rotundifolia*) in Florida and the second detection of this nematode on the genus *Vitis* in North America. Although the known host range for *P. hippeastri* in Florida, is narrow and includes amaryllis (Inserra et al., 2007), bromeliads, bottlebrush (*Callistemon rigidus*) (De Luca et al., 2010), St. Augustingrass

(*Stenotaphrum secundatum*) and bermudagrass (*Cynodon dactylon*) (William Crow, personal communication), the recovery of *P. hippeastri* from muscadine grape and other hosts outside Florida (Chen et al., 2014; Gu et al. 2014; Wang et al. 2016; Shokoohi et al. 2019; Snoetze et al. 2019; Handoo et al., 2020) suggests that its host range is much wider than previously reported. However, the economic impact of *P. hippeastri*'s infection on muscadine grape in Florida remains undetermined.

## LITERATURE CITED

- Anderson, P. C., A. Sarkhosh, D. Huff, and J. Breman. 2003. The Muscadine Grape (*Vitis rotundifolia* Michx. UF/IFAS Extension (HS763), Revised October 2020, Gainesville, FL.
- Castillo, P., and N. Vovlas. 2007. *Pratylenchus* (Nematoda: Pratylenchidae): Diagnosis, Biology, Pathogenicity and Management. Nematology Monographs and Perspectives. The Netherlands-USA: Brill Leiden-Boston.
- Chen, W. J., Y. Bian, R. Wu, X. J. Lin, M. Z. Zhang, Z. Y. Wu, Y. Wu, X. Y. Wu, and X. Chen. 2014. Root-lesion nematode, *Pratylenchus hippeastri*, on *Acer palmatum* imported from Japan. *Acta Agriculturae Zhejiangensis* 26:708-713.
- Crow, T., and J. R. Rich. 2006. Nematodes of backyard deciduous fruit and nut crops in Florida. UF/IFAS Extension (ENY-055), Revised June 2017, Gainesville, FL.
- Crow, W. T., A. Habteweld, and T. Bean. 2020. Mist chamber extraction for improved diagnosis of *Meloidogyne* spp. from golf course bermudagrass. *Journal of Nematology* 52:1-12.
- De Ley, P., I. Tandingan De Ley, K. Morris, E. Abebe, M. Mundo-Ocampo, M. Yoder, J. Heras, D. Waumann, A. Rocha-Olivares, A. H. J. Burr, J. G. Baldwin, and W. K. Thomas. 2005. An integrated approach to fast and informative morphological vouchering of nematodes for applications in molecular barcoding. *Philosophical Transactions of the Royal Society B* 360:1945-58.
- De Luca, F., A. Troccoli, L. W. Duncan, S. A. Subbotin, L. Waeyenberge, M. Moens, and R. N. Inserra. 2010. Characterization of a population of *Pratylenchus hippeastri* from bromeliads and description of two related new

- species, *P. floridensis* n. sp. and *P. parafloridensis* n. sp., from grasses in Florida. *Nematology* 12:847–68.
- Derycke, S., T. Remerie, A. Vierstraete, T. Backeljau, J. Vanfleteren, M. Vincx, and T. Moens. 2005. Mitochondrial DNA variation and cryptic speciation within the free-living marine nematode *Pellioiditis marina*. *Marine Ecology-Progress Series* 300:91–103.
- Duncan, L. W., R. N. Inserra, and D. Dunn. 1998. Seasonal changes in citrus root starch concentration and body length of female *Pratylenchus coffeae*. *Nematropica* 28:263–266.
- Gu, J. F., N. Wang, J. He, and W. J. Chen. 2014. Identification of *Pratylenchus hippeastri* from imported seedlings. *Plant Quarantine* 28:41–46.
- Habteweld, A., F. Akyazi, S. Joseph, W. T. Crow, E. Abebe, and T. Mekete. 2019. Description of *Hirschmanniella dicksoni* n. sp. (Nematoda: Pratylenchidae) from rhizosphere soil of limpograss from Florida, USA. *Journal of Nematology* 51:1–15.
- Handoo, Z., A. M. Skantar, M. R. Kantor, S. L. Hafez, and M. N. Hult. 2020. Molecular and morphological characterization of the amaryllis lesion nematode, *Pratylenchus hippeastri* (Inserra *et al.*, 2007), from California. *Journal of Nematology* 52:1–5.
- Howland, A. D., R. P. Schreiner, and I. A. Zasada. 2014. Spatial distribution of plant-parasitic nematodes in semi-arid *Vitis vinifera* vineyards in Washington. *Journal of Nematology* 46:321–330.
- Inserra, R. N., A. Troccoli, U. Gozel, E. C. Bernard, D. Dunn, and L. W. Duncan. 2007. *Pratylenchus hippeastri* n. sp. (Nematoda: Pratylenchidae) from amaryllis in Florida with notes on *P. scribneri* and *P. hexincisus*. *Nematology* 9:25–52.
- Janssen, T., G. Karssen, V. Orlando, S. A. Subbotin, and W. Bert. 2017. Molecular characterization and species delimiting of plant-parasitic nematodes of the genus *Pratylenchus* from the *penetrans* group (Nematoda: Pratylenchidae). *Molecular Phylogenetics and Evolution* 117:30–48.
- Knoetze, R., E. Van den Berg, C. Girgan, and L. van der Walt. 2019. First report of the root lesion nematode, *Pratylenchus hippeastri*, on apple in South Africa. *Journal of Plant Diseases and Protection* 126:607–609.
- Kumar, S., G. Stecher, M. Li, C. Knyaz, and K. Tamura. 2018. MEGA X: Molecular evolutionary genetics analysis across computing platforms. *Molecular Biology and Evolution* 35:1547–1549.
- Landa, B. B., J. E. P. Rius, N. Vovlas, R. Carneiro, C. M. N. Maleita, I. M. D. Abrantes, and P. Castillo. 2008. Molecular characterization of *Meloidogyne hispanica* (Nematoda, Meloidogynidae) by phylogenetic analysis of genes within the rDNA in *Meloidogyne* spp. *Plant Disease* 92:1104–10.
- Pagan, C., D. Coyne, R. Carneiro, G. Kariuki, N. Luambana, A. Affokpon, and V. M. Williamson. 2015. Mitochondrial haplotype-based identification of ethanol-preserved root-knot nematodes from Africa. *Phytopathology* 105:350–357.
- Shokoohi, E., J. Abolafia, P. W. Mashela and N. Divsalar. 2019. New data on known species of *Hirschmanniella* and *Pratylenchus* (Rhabditida, Pratylenchidae) from Iran and South Africa. *Journal of Nematology* 51:1–26.
- Tamura K., and M. Nei. 1993. Estimation of the number of nucleotide substitutions in the control region of mitochondrial DNA in humans and chimpanzees. *Molecular Biology and Evolution* 10:512–526.
- Téliz, D., B. B. Landa, H. F. Rapoport, F. P. Camacho, R. M. Jiménez-Díaz, and P. Castillo. 2007. Plant-parasitic nematodes infecting grapevine in southern Spain and susceptible reaction to root-knot nematodes of rootstocks reported as moderately resistant. *Plant Disease* 91:1147–1154.
- Wang, H. H., K. Zhuo, and J. L. Liao. 2016. Morphological and molecular characterization of *Pratylenchus hippeastri*, a new record of root lesion nematode associated with apple in China. *Pakistan Journal of Zoology* 48:665–71.

---

Received:

2/XIII/2021

Accepted for publication:

28/IX/2021

Recibido:

Aceptado para publicación: